Cell

Amyloid-like Aggregates Sequester Numerous Metastable Proteins with Essential Cellular Functions

Heidi Olzscha,[1,4] Sonya M. Schermann,[1,4] Andreas C. Woerner,[1] Stefan Pinkert,[1] Michael H. Hecht,[2] Gian G. Tartaglia,[3,5] Michele Vendruscolo,[3] Manajit Hayer-Hartl,[1,*] F. Ulrich Hartl,[1,*] and R. Martin Vabulas[1,*]

[1]Department of Cellular Biochemistry, Max Planck Institute of Biochemistry, Am Klopferspitz 18, D-82159 Martinsried, Germany
[2]Department of Chemistry, Princeton University, Princeton, NJ 08544, USA
[3]Department of Chemistry, University of Cambridge, Lensfield Road, Cambridge CB2 1EW, UK
[4]These authors contributed equally to this work
[5]Present address: Bioinformatics & Genomics Program, CRG Centre for Genomic Regulation, Dr. Aiguader 88, Barcelona 08003, Spain
*Correspondence: mhartl@biochem.mpg.de (M.H-H.), uhartl@biochem.mpg.de (F.U.H.), vabulas@biochem.mpg.de (R.M.V.)
DOI 10.1016/j.cell.2010.11.050

SUMMARY

Protein aggregation is linked with neurodegeneration and numerous other diseases by mechanisms that are not well understood. Here, we have analyzed the gain-of-function toxicity of artificial β sheet proteins that were designed to form amyloid-like fibrils. Using quantitative proteomics, we found that the toxicity of these proteins in human cells correlates with the capacity of their aggregates to promote aberrant protein interactions and to deregulate the cytosolic stress response. The endogenous proteins that are sequestered by the aggregates share distinct physicochemical properties: They are relatively large in size and significantly enriched in predicted unstructured regions, features that are strongly linked with multifunctionality. Many of the interacting proteins occupy essential hub positions in cellular protein networks, with key roles in chromatin organization, transcription, translation, maintenance of cell architecture and protein quality control. We suggest that amyloidogenic aggregation targets a metastable subproteome, thereby causing multifactorial toxicity and, eventually, the collapse of essential cellular functions.

INTRODUCTION

The majority of proteins must fold into well-defined three-dimensional structures in order to fulfill their biological functions. This fundamental process is aided by a complex cellular machinery of molecular chaperones, which act to prevent misfolding and aggregation (Frydman, 2001; Hartl and Hayer-Hartl, 2002; Morimoto, 2008). Failure of a protein to fold properly, or to retain its folded state, has emerged as the cause of numerous diseases. Aberrant folding is often the result of destabilizing mutations and may cause the loss of critical functions. However, in a growing number of diseases, misfolding and aggregation results predominantly in a toxic gain of function (Stefani and Dobson, 2003; Winklhofer et al., 2008). In these disorders, specific proteins, differing substantially in size and sequence, typically self-assemble into amyloid-like fibrils with cross-β structure which are deposited within or outside of cells. This phenomenon underlies some of the most debilitating neurodegenerative disorders, including Parkinson's, Huntington's, and Alzheimer's disease.

Amyloidogenic aggregation is observed with many protein sequences (Chiti and Dobson, 2006; Goldschmidt et al., 2010) and is often associated with the accumulation of soluble, oligomeric species that precede fibril formation and are thought to be responsible for toxicity (Campioni et al., 2010; Chiti and Dobson, 2006; Jahn and Radford, 2008). The underlying mechanisms are only poorly understood but a prominent hypothesis suggests that the aggregates, in particular the more heterogeneous oligomers, may expose flexible hydrophobic surfaces that can mediate aberrant interactions with other proteins, resulting in their functional impairment and sequestration (Bolognesi et al., 2010; Chiti and Dobson, 2006). In another model, misfolding proteins, by engaging the chaperone machinery, are thought to interfere with central protein quality control and clearance mechanisms, possibly resulting in a propagation of folding defects (Balch et al., 2008; Bence et al., 2001; Gidalevitz et al., 2006). Finally, based on experiments with model membranes, oligomeric aggregation intermediates can compromise the integrity of lipid membranes (Lashuel and Lansbury, 2006). Importantly, these different routes of toxic action are not mutually exclusive but may operate in parallel.

To investigate the toxicity mechanisms of amyloid-like aggregation, we have established a cellular model based on the expression of artificial proteins that were designed to form β sheet structures, and shown previously to self-assemble into fibrils in vitro (West et al., 1999). The sequences of these proteins were explicitly designed to contain β strands with an alternating pattern of polar and nonpolar residues, while the exact identities of the side chains were varied combinatorially. Similar bipolar

segments occur in ~30% of human proteins, including several neurodegenerative disease proteins, but are usually buried within the folded structure (Tartaglia et al., 2008). Because the model proteins were designed de novo, they are not biased by the evolutionary burden of natural proteins and thus allowed us to study the gain-of-function toxicity caused by aggregation without interference either from loss-of-function alterations or from an augmentation of the biological activities of natural disease proteins (Cooper et al., 2006; Lam et al., 2006).

Here, we tested specifically the hypothesis that the aggregates engage in widespread aberrant protein interactions. We found that expression of the model proteins in human cells results in aggregate formation and toxicity. Quantitative proteomic analysis reveals that the aggregates interact with and sequester multiple preexistent and newly synthesized proteins. Interestingly, these interactions can be explained in terms of specific sequence features of the coaggregating proteins, such as their multidomain character and their enrichment in disordered regions, properties that are strongly linked with multifunctionality and the occupancy of hub positions in the cellular protein network. We suggest that aberrant interactions with numerous proteins having key cellular functions contribute to aggregate toxicity.

RESULTS

Designed β Sheet Proteins Are Cytotoxic

To investigate the gain-of-function cytotoxicity associated with amyloid-like aggregation, we used several model polypeptides from a combinatorial library rationally designed to form cross-β fibrils (West et al., 1999). These proteins, henceforth designated as β proteins, contain six β strands connected by 4-amino acid linker segments, with each strand comprising seven amino acids in a polar-nonpolar alternating pattern. An N-terminal c-Myc-epitope was attached to facilitate detection (Figure 1A). The three proteins chosen for analysis, β4, β17, and β23, differ in sequence (pairwise identities of β strands ~35%), with β23 having the highest hydrophobic volume and β sheet propensity, due to its higher isoleucine content (Figure 1A) (Tartaglia et al., 2008). As a control, we used the designed α-helical protein, α-S824, which is similar to the β proteins in amino acid composition but folds into a 4-helix bundle structure (Wei et al., 2003) (Figure 1A).

Upon dilution from denaturant into physiological buffer, the purified β proteins adopted β sheet conformation as determined by CD and rapidly assembled into aggregates detectable with the amyloid-binding dyes thioflavin T (ThT) and NIAD-4 (Nesterov et al., 2005) (Figures 1B, 1C, and Figures S1A and S1B available online). The intensity of ThT and NIAD-4 binding was highest for β23, followed by β17 and β4 (Figures 1B and 1C), consistent with the relative β aggregation propensity of these proteins calculated with the sequence-based Z^{agg} method (Tartaglia et al., 2008) (Z^{agg} scores are: β4, 0.79; β17, 0.83; β23, 0.93; α-S824, and 0.30). ANS fluorescence, a probe for exposed hydrophobic regions, suggested the presence of hydrophobic surfaces on the aggregates, in particular for β23 and β17 (Figure 1D). As shown via electron microscopy, the β proteins formed mostly relatively short protofilaments (~2–3 nm in diameter) as well as more heterogeneous, globular aggregates (Figure 1E). Formation of globular species was most pronounced with β23 (Figure 1E). Similar prefibrillar aggregates are also observed with natural amyloidogenic proteins and correlate with cytotoxicity (Bolognesi et al., 2010; Campioni et al., 2010; Chiti and Dobson, 2006). In contrast, in low-salt buffer (pH 6), the β proteins formed thicker (10–12 nm diameter) and longer fibrils (Figure 1F) with FTIR spectroscopic properties characteristic of amyloid (Figure S1C). Thus, the model proteins undergo amyloid-like aggregation in vitro, and in physiological buffer populate prefibrillar species.

Upon expression in HEK293T cells for 3 days, the β proteins, but not α-S824, reduced cell viability substantially, as measured by the MTT assay (Figure 2A), and induced cell death in the order β23 > β17 > β4 (Figures S2A and S2B). Cell viability was less impaired after 24 hr of expression, without a significant difference in toxicity between the three β proteins (Figure 2A). Upon cell fractionation, the β proteins were largely recovered in the insoluble fraction, whereas α-S824 was soluble (Figure 2B). Note that β4 and β17 migrated on SDS-PAGE more slowly than expected, but this difference was not observed in urea/SDS gels (Figure S1A). Confocal immunofluorescence microscopy with anti-Myc antibody showed that the β-protein-expressing cells adopted a collapsed shape lacking filopodia (Figure 2C). Aggregates accumulated mostly in the perinuclear space and the nuclei were often deformed. The aggregates were NIAD-4 positive (Figure 2D), suggesting the presence of amyloid-like material. To detect oligomeric aggregation intermediates, cell extracts were fractionated by size exclusion chromatography followed by dot blot analysis with the A11 antibody, which was raised against the Alzheimer Aβ peptide and preferentially recognizes amyloid oligomers associated with cytotoxicity, independent of amino acid sequence (Kayed et al., 2003). β23 expression generated substantially higher levels of A11 reactive material than expression of β4 and β17 (Figure 2E and Figure S2C), consistent with the greater toxicity of β23 and its pronounced tendency to form prefibrillar aggregates in vitro (Figures 1E and 1F).

In summary, the designed β proteins resemble amyloidogenic disease proteins in terms of aggregation properties and toxicity and allow us to investigate the mechanism of gain-of-function toxicity independently from evolved biological interactions.

Identification of the β Protein Interactome

Gain-of-function toxicity of aggregation may arise, at least in part, from aberrant interactions of the aggregates with cellular proteins. To test this hypothesis, we performed a sensitive, quantitative proteomic analysis of the β protein interactome using SILAC (stable isotope labeling with amino acids in cell culture) (Ong and Mann, 2006) and peptide identification by tandem mass spectrometry (LC-MS/MS). These experiments were performed at 24 hr after β protein transfection when cell viability was not yet severely impaired (Figure 2A). In one set of experiments, cells labeled with light (L), medium (M) or heavy (H) arginine and lysine isotopes were transfected with empty vector, α-S824 and β23, respectively. In another set-up, α-S824, β4, and β17 were expressed in L-, M-, and H-labeled cells, respectively (Figure 3A). Preferential interactions with β4,

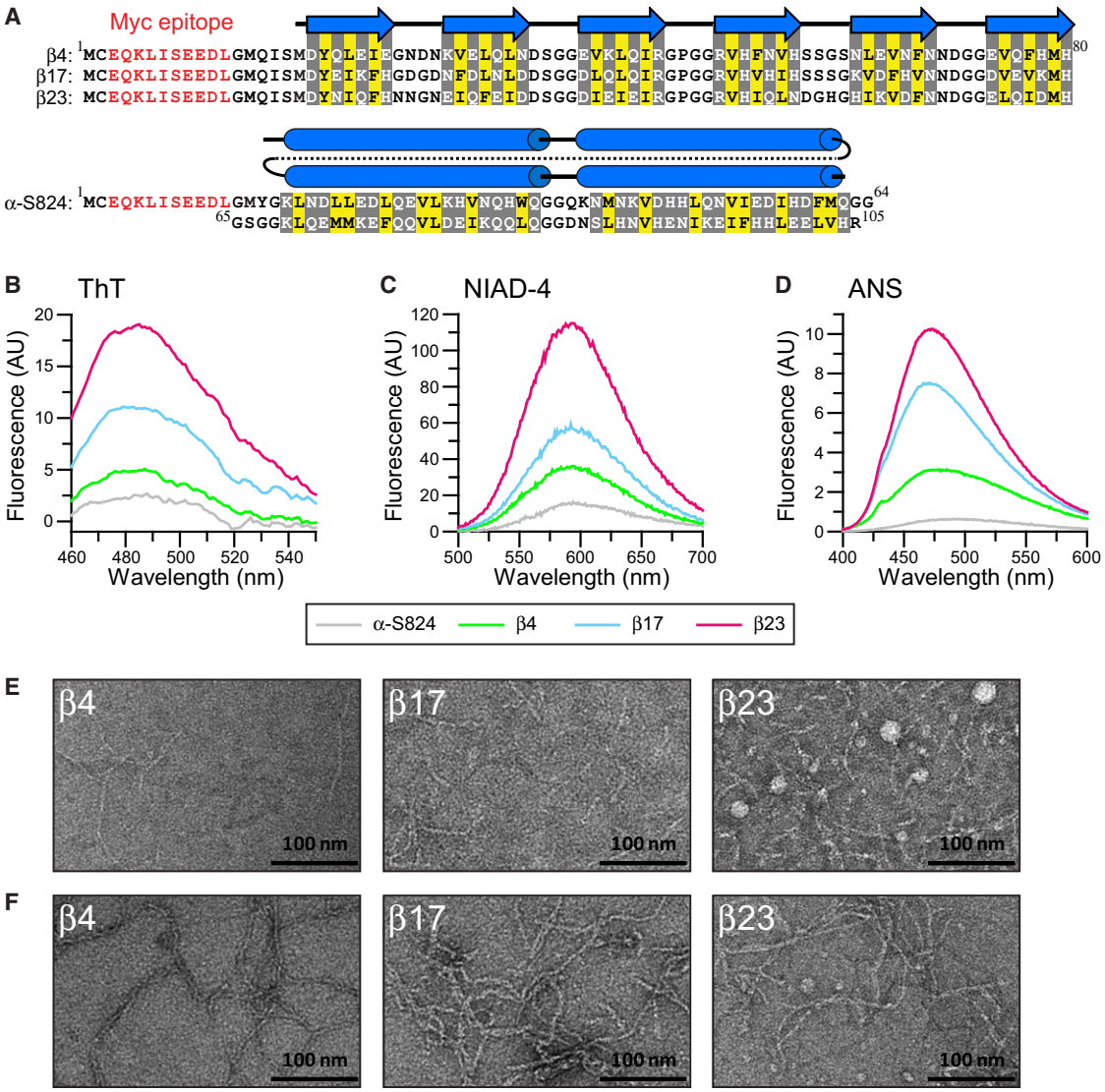

Figure 1. Amyloidogenic Aggregation of Model Proteins In Vitro

(A) Sequences of the model proteins, β4, β17, and β23, designed to form β-sheet fibrils, and α-S824 designed to form a 4-helical bundle. Polar and nonpolar amino acids are indicated in gray and yellow, respectively, β strands and α helices by blue arrows and rods respectively. N-terminal c-Myc tags are shown in red.

(B–D) Tinctorial properties of β protein aggregates. The purified proteins indicated (3 μM) were analyzed in 25 mM HEPES buffer (pH 7.5), 150 mM KCl, 0.5 mM $MgCl_2$-containing 20 μM Thioflavin T (B), 1 μM NIAD-4 (C), or 20 μM ANS (D). Fluorescence was recorded as described in Experimental Procedures.

(E and F) Transmission electron microscopy of aggregates formed by β4, β17 and β23, as above, at pH 7.5 (E) or 10 mM potassium phosphate (pH 6.0) (F). Proteins were negatively stained and observed at a magnification of 55,000×.

See also Figure S1.

β17, or β23 were explored in a third type of experiment. Total cell lysates were prepared essentially without removal of aggregate material and combined 1:1:1 (Figure 3A and Figure S3A). The expressed proteins were quantitatively isolated using anti-Myc antibody coupled to magnetic beads, followed by SDS-PAGE, in-gel digestion, and LC-MS/MS analysis.

It seemed plausible that initial coaggregation may be driven by relatively weak interactions, which might introduce a stochastic element in the proteomic analysis. To overcome this problem we based our analysis on extensive biological repetitions of the experiments. Three proteomic experiments were performed, each consisting of three biological repeats (independent transfections). A protein was identified as β protein interactor when its isotope-labeled peptides were either enriched relative to the α-S824 control or relative to one of the other β proteins with > 95% confidence in at least two of the three repeats of a set (see Extended Experimental Procedures and Figures S3B–S3D). A total of 94 interactors of β23, 73, of β17 and 57 of β4 were identified in experiments of equivalent sampling size, consistent with the relative toxicity of the proteins (Figure 3B

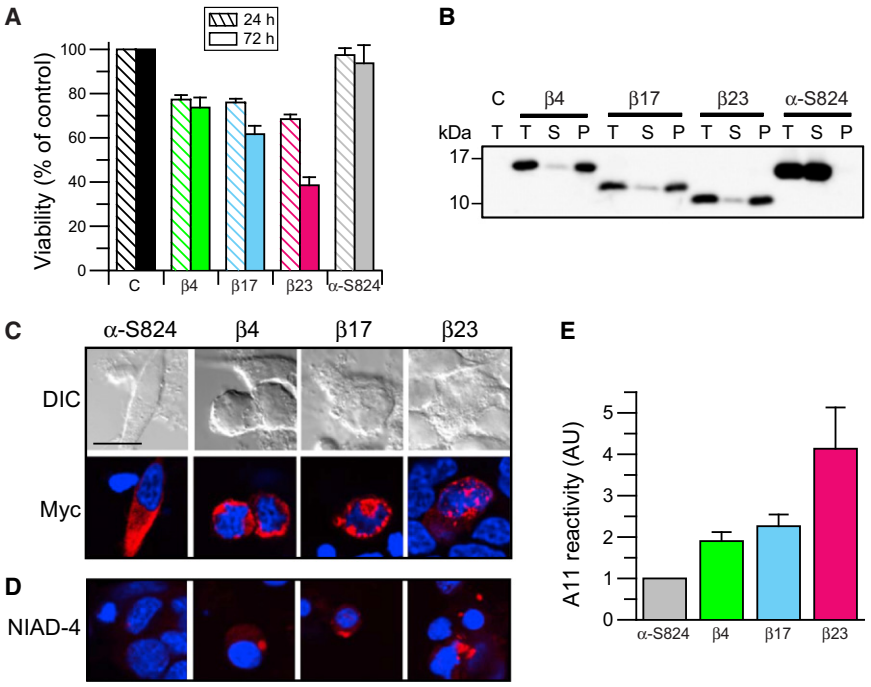

Figure 2. Cytotoxicity and Aggregation of Model Proteins in HEK293T Cells

(A) Viability of HEK293T cells expressing β4, β17, β23, and α-S824 measured by MTT assay 24 hr and 72 hr after transfection. MTT reduction by control cells transfected with empty vector, C, was set to 100%. Standard deviations were derived from at least three independent experiments.

(B) Solubility of β4, β17, β23, and α-S824 analyzed by fractionation of lysates from cells 24 hr after transfection by centrifugation and immunoblotting with anti-Myc antibody. T, total lysate; S, soluble fraction; P, pellet fraction; C, empty vector control. Representative results from at least three independent experiments.

(C and D) Protein distribution and aggregation in intact cells expressing α-S824, β4, β17, and β23. After 24 hr, proteins were detected by immunofluorescence with anti-Myc antibodies (C). DIC, differential interference contrast images. Amyloid-like aggregates were detected by staining with NIAD-4 (D) (see Experimental Procedures). Nuclei were counterstained with DAPI. The scale bar represents 20 μm. Representative images of three independent experiments.

(E) Quantification of A11 antibody reactivity in extracts from β-protein-expressing cells 24 hr after transfection. The cumulative dot blot signal of fractions from size exclusion chromatography was corrected for the cumulative anti-Myc signal, indicating the amounts of α-S824, β4, β17, and β23, and expressed relative to the A11 reactivity in α-S824 expressing cells (set to 1) (see Figure S2C for original data). Averages and standard deviations represent at least three independent experiments.

See also Figure S2.

and Tables S1–S3). Only four proteins were marginally enriched on α-S824 relative to the vector only control, including two ribosomal proteins (Figure S3B). Approximately 60% of the β4 and β17 interactors were also found to interact with β23, indicating a high degree of overlap in interaction profiles (Figure 3B). Western blotting of pulldowns and immunofluorescence analysis of cells confirmed the results from SILAC/MS for several interactors (Figures S3E and S3F). Thus, interactions of the β protein aggregates with multiple endogenous proteins precede the strong decrease in cell viability observed at 72 hr after transfection (Figure 2A).

As summarized for β23, most of the proteins associated with the aggregates have their primary location in the cytoplasm, nucleus and mitochondria (Figure 3C and Table S1). Proteins involved in chromatin regulation, RNA processing, transcription, translation, cytoskeletal function, vesicle transport, and protein quality control were highly represented. These proteins are generally of average cellular abundance (Su et al., 2002) and for several of them between 10% and 45% of total was associated with the aggregates, based on depletion from supernatant fractions after pulldown as measured by SILAC/MS (Table S1 and Extended Experimental Procedures). Note that this analysis probably underestimates the extent of sequestration, since coaggregates may partially dissociate during isolation. Interestingly, 12 different translation initiation factors interacted directly or indirectly with the aggregates, including 9 of the 13 subunits of the eIF3 complex and 3 subunits of eIF4 (Figure 3C). β17 aggregates contained 10 and β4 aggregates 9 of these proteins (Tables S2 and S3). Immunofluorescence analysis demonstrated extensive co-localization of eIF3D and eIF4GII with the aggregates and western blotting of pulldowns confirmed that at least ~10% of cellular eIF3D coaggregated with β23 and β17, compared to ~6% with β4 (Figures S3E and S3F, and data not shown). Indeed, labeling experiments showed that cells expressing β23 for 24 hr had a ~35% reduced protein synthesis capacity (Figure S3G). Similarly, the altered morphology of β-protein-expressing cells revealed by actin staining (Figure S3H) may be attributed to the association of filamins A, B, C, (FLNA, FLNB, FLNC), and the giant protein plectin-1 (PLEC1) (~500 kDa) with the aggregates (Figure 3C), proteins that are critical for the formation and maintenance of cytoskeletal architecture. These results show that many different proteins, involved in a range of essential cellular functions, are affected by the β protein aggregates.

Aberrant Stress Response in β-Protein-Expressing Cells

The proteomic analysis identified several cytosolic chaperones and chaperone regulators to be associated with the aggregates, including Hsc70 (Hsc71) and its cochaperones Hsp110 (Hsp105), Hdj1/2 and Bag2, as well as the nascent chain associated complex, NAC (Figure 3C). Hsp110 was enriched in the aggregates in a manner correlating with the relative toxicity of β4, β17 and β23, as confirmed by western blotting and immunofluorescence (Figures 4A and 4B). Indeed, overexpression of Hsp110 (Figure S4A) partially suppressed β4 and β17 aggregation and toxicity but was inefficient in mitigating the toxic effects of β23 (Figures 4C and Figures S4B and S4C).

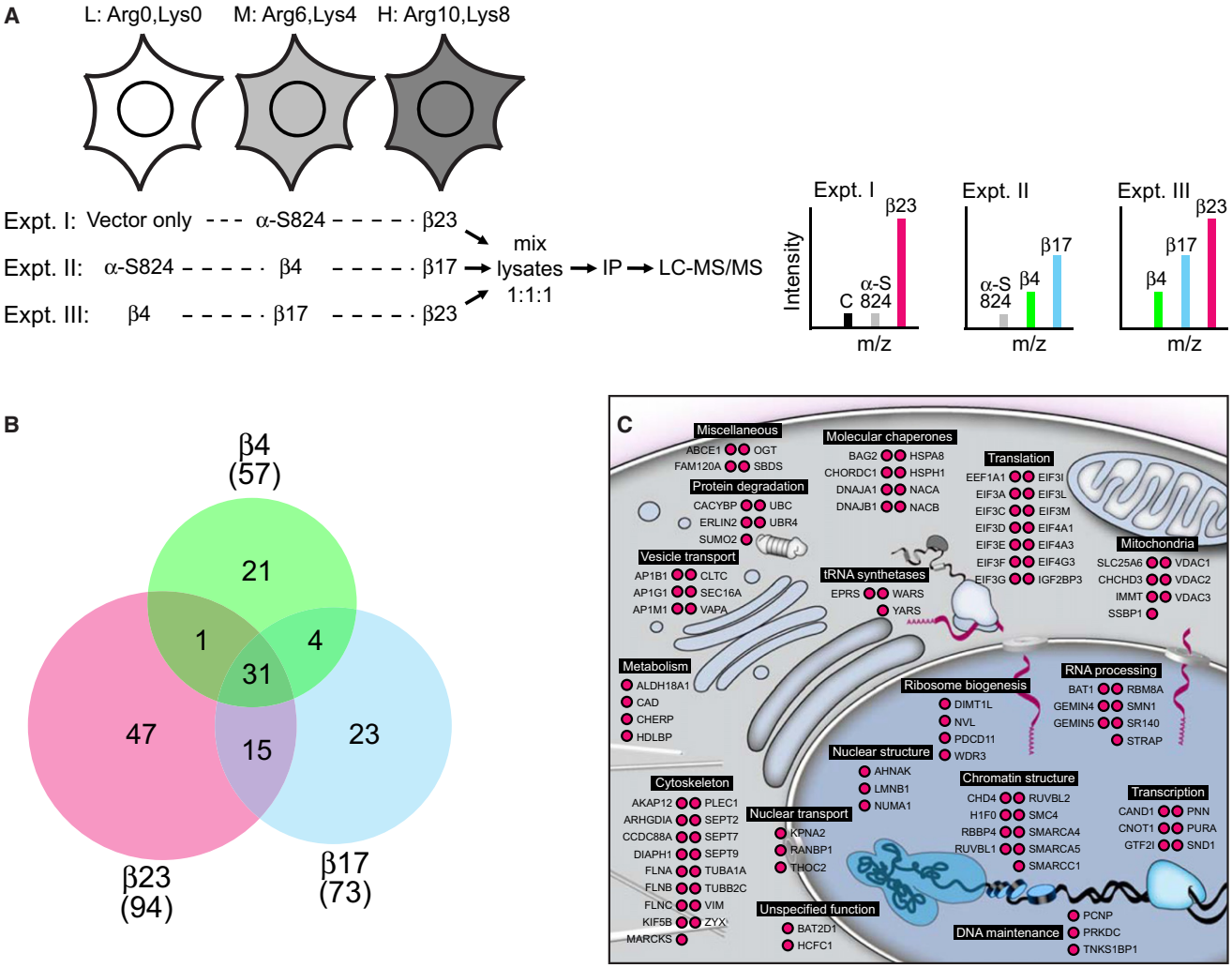

Figure 3. Interactome Analysis of β proteins

(A) Design of SILAC experiments to identify β protein interactors by LC-MS/MS. L, M, and H, light, medium, and heavy isotope media. C, vector only control.

(B) Overlap between the interactor sets of β4, β17, and β23. Total numbers of identified interactors are given in parentheses.

(C) The β23 interacting proteins are grouped according to cellular location and function.

See also Figure S3 and Tables S1–S3.

Remarkably, expression of the β proteins did not induce the cytosolic stress response or heat-shock response (HSR), as no increase in the levels of Hsp110, Hsp70, or Hsp27 was observed (Figures 4A and data not shown). A possible defect in the HSR was further analyzed using a luciferase reporter gene under control of the HSF1-dependent Hsp70 promoter (Williams et al., 1989). While inhibition of proteasome function by MG132 in control cells resulted in a 5-fold induction of the reporter, this induction was completely abolished in cells expressing the β proteins for 24 hr (Figure 4D). The phorbol-12-myristate-13-acetate (PMA)-mediated induction of a luciferase reporter under the NF-κB promoter was also impaired, but to a lesser extent than the inhibition of the stress response (Figure 4E). Thus, expression of the model β sheet proteins leads to a deficiency of the normal cytosolic stress response, thereby limiting the capacity of cells to mount an effective defense.

Structural Features of β Protein Interactors

A bioinformatic analysis of the physicochemical properties of the β protein interactors was conducted to see whether these proteins share certain structural features. We focused our initial analysis on the interactors of β23 (Table S1). Compared to a set of 3055 control proteins identified by LC-MS/MS in a total cell lysate (Table S4), the β23 interactors are shifted to higher molecular weight, with a significantly greater fraction of proteins above 150 kDa ($p < 0.005$) (Figure 5A). In addition, the interactors have a lower average hydrophobicity and a bimodal hydrophobicity distribution (Kyte and Doolittle, 1982) ($p < 0.005$) (Figure 5B). The occurrence of domain folds among the β23 interactors, as classified in SCOP, was generally similar to that of lysate proteins. However, the β23 interactors contained significantly more proteins with all beta domains (SCOP class b) ($p < 0.05$) (Figure S5A), including the beta-barrel VDAC proteins of the

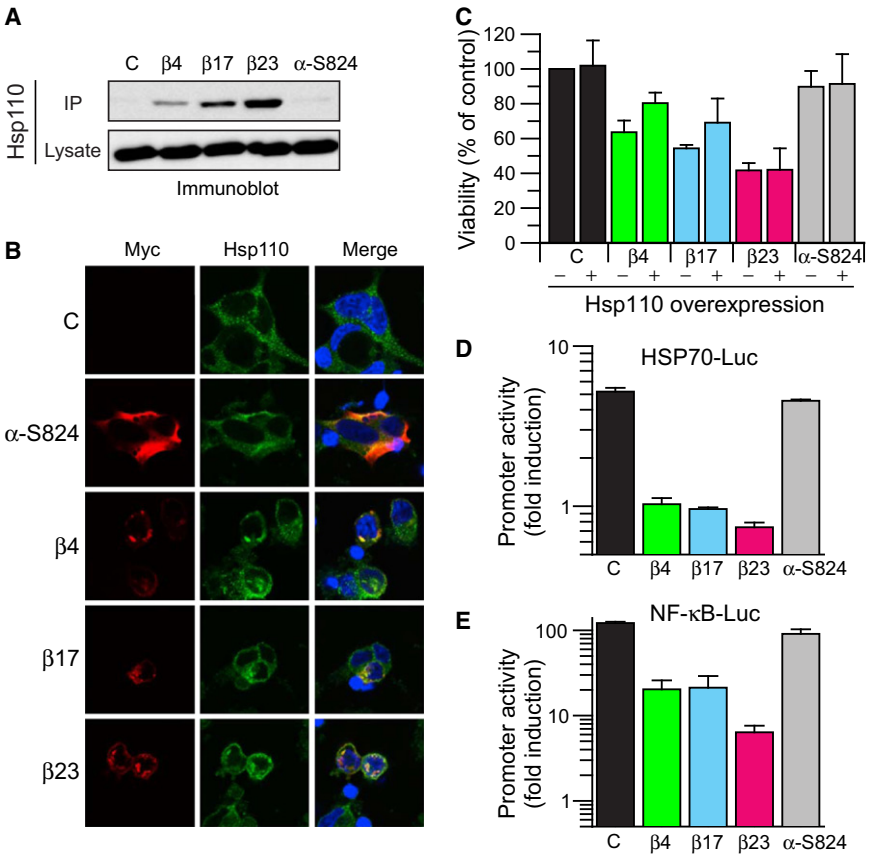

Figure 4. Impairment of the Stress Response in β-Protein-Expressing Cells

(A and B) Association of Hsp110 with β protein aggregates. HEK293T cells were transfected as indicated (C, empty vector control). 24 hr after transfection, Myc-tagged proteins β4, β17, β23, and α-S824 were immunoprecipitated from cell lysates and analyzed by immunoblotting with anti-HSP110 antibody (A). Lysate samples correspond to 8% of input used for IP. β4, β17, and β23 in pulldowns was associated with ~5%, 9%, and 16% of total cellular Hsp110, respectively (also see Figure S3F). For immunofluorescence analysis (B), cells were fixed and costained with anti-Myc antibodies and anti-Hsp110 antibodies. Nuclei were stained with DAPI. Representative examples of three independent experiments are shown.

(C) Partial rescue of β protein toxicity by Hsp110 overexpression. Cells were transfected with empty vector or the expression vector for human Hsp110. 24 hr later, cells were electroporated with empty vector, C, or expression vectors for β4, β17, β23, and α-S824. Three days after the second transfection, MTT assays were performed. Empty vector control was set to 100% viability. Standard deviations of three independent experiments are shown.

(D and E) Inhibitory effect of β proteins on cellular stress response pathways. Cells were cotransfected with HSP70-luciferase reporter (D) or NF-κB-luciferase reporter constructs (E) and the β-protein-expressing plasmids. 6 hr later, 5 μM MG132 (D) or 16 μM PMA (E) were added to induce the respective promoter. Luciferase activity was measured 24 hr after transfection. The promoter activity in cells transfected with control vector, C, without inducer was set to 1. Standard deviations of three independent experiments are shown.

See also Figure S4.

outer mitochondrial membrane and the filamins which have Ig-domain repeats (Table S1 and Figure S3F).

The lower hydrophobicity of many interactors suggested that these proteins may be rich in intrinsically unstructured regions (IURs). Indeed, compared to lysate proteins, the β23 interactors have a significantly greater fraction of total amino acids in IURs ($p < 0.05$), based on the DisoDB database (Pentony and Jones, 2009) and the DisEMBL and IUPred prediction tools for unstructured regions (Dosztanyi et al., 2005; Linding et al., 2003) (Figure 5C, Tables S1 and S4, and data not shown). Pronounced differences emerged when considering the fraction of proteins with IURs longer than 30 or 50 residues (Figure 5D). For example, ~60% of the β23 interactors are predicted to contain at least one unstructured segment of 30 amino acids, compared to ~45% in lysate proteins or the complete proteome ($p < 0.005$) (Figure 5D). The corresponding numbers for IURs > 50 amino acids are ~40% and ~25% ($p < 0.005$), respectively. Moreover, the β23 interactors contain on average ~3 disordered segments of 30 amino acids (compared to ~1.8 for the lysate proteins, $p < 0.005$). The predicted IURs of the interactors are shifted to greater length ($p < 0.005$) (Figure S5B and Tables S1 and S4), with 21% of the proteins containing IURs > 80 amino acids and 10% of 100 to 429 residues. The IURs are enriched in polar amino acids and in amino acids that have a high propensity to form coil and turn regions, such as M, K, R, E, S, Q, and P, and are depleted in aromatic and hydrophobic amino acids W, Y, F, C, I, and V (Dunker et al., 2008). Such sequences are structurally flexible and populate a range of conformational states from extended disordered to collapsed, molten globule-like structures (Dunker et al., 2008; Pentony and Jones, 2009). Using the Z^{agg} algorithm to predict aggregation propensities, the β23 interactors have higher aggregation scores than lysate proteins (see Figure S6B below).

A comparison of the proteins that interact preferentially with β4, β17, and β23 (18, 28, and 27 proteins, respectively), as defined by the SILAC experiments (Figure S3D and Extended Experimental Procedures), revealed that a gradual increase in molecular weight and decrease in hydrophobicity of the interactors, along with a slight increase in their disorder, correlated with the differential cytotoxicity of the three β proteins (Figure 5E). This trend was also observed when comparing the complete interactor sets of the three β proteins (Tables S1–S3).

The prominent association of proteins with low hydrophobicity and high intrinsic disorder with the aggregates was

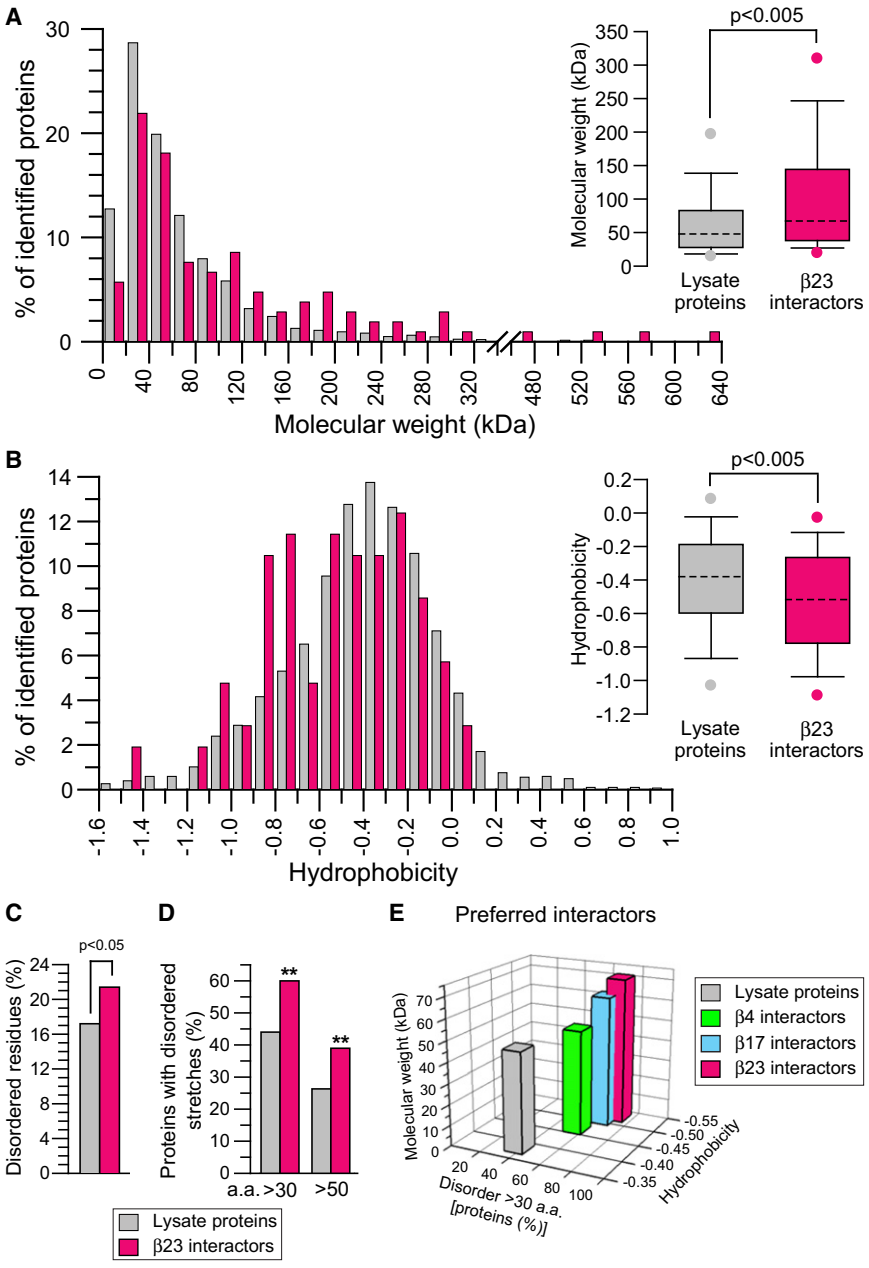

Figure 5. Structural Properties of the β Protein Interactors

(A and B) Distribution of molecular weight (A) and average hydrophobicity (B) of lysate proteins (gray) and β23 interactors (red) (Tables S1 and S4). Box plots (insets) indicate the distribution of the data. Dashed horizontal line indicates the median, whisker caps and circles indicate 10th/90th and 5th/95th percentiles, respectively. P values are based on Mann-Whitney test.

(C and D) Disorder analysis of β protein interactors. Percentage of disordered residues in interactor sequences (C). p value based on Mann-Whitney test. Fraction of proteins with disordered stretches longer than 30 or 50 amino acids (D). **p < 0.005 based on a chi-square test. Disorder was determined using DisoDB.

(E) Structural properties of lysate proteins and of proteins interacting preferentially with β4, β17, or β23.

See also Figure S5 and Tables S1–S6.

unexpected. To test whether such proteins are targeted more generally by amyloid-like aggregation, we performed an initial analysis of interactors of wild-type $A\beta_{1-42}$ and its Arctic mutant (E22G), which causes early-onset Alzheimer's disease. The latter was included because it is known to populate higher levels of prefibrillar aggregates and toxic oligomers exposing hydrophobic surfaces (Bolognesi et al., 2010; Nilsberth et al., 2001). To allow a comparison with the model β aggregates, the Aβ proteins were also expressed in the cytosol, using GFP fusions (Kim et al., 2006). In contrast to the artificial β proteins, the Aβ constructs were degraded but accumulated upon partial proteasome inhibition with MG132 (Figure S5C) (Lee et al., 2006). The Arctic mutant formed visible aggregates more readily and showed substantially greater toxicity than WT $A\beta_{1-42}$ (Figures S5D and S5E). Analysis by SILAC/MS revealed that the Aβ interactome is comparable in complexity to that of the β proteins, with a direct overlap of ~25%, prominently including translation initiation factors, chromatin regulators, RNA processing proteins, mitochondrial membrane proteins and chaperones (Table S5). We also identified 31 proteins which were enriched on the Arctic mutant relative to the less toxic $A\beta_{1-42}$ WT (Table S6). Notably, these proteins resemble the β protein interactors in physicochemical properties and are significantly enriched in IURs ($p < 0.05$) (Figures S5F–S5I).

From these results, we conclude that cells contain a subpopulation of metastable proteins that are prone to interact with and potentially become sequestered by toxic species populated in the process of amyloid-like aggregation.

β Protein Interactors Include Pre-Existent and Newly Synthesized Proteins

While the results above suggested that structural flexibility is critical in facilitating the interaction of endogenous proteins with the β aggregates, we noted that for ~40% of the β23 interactors no IURs > 30 amino acids are predicted (Figure 5D and Table S1). We therefore considered the possibility that some of these proteins may succumb to coaggregation upon synthesis before adopting stably folded structures. To test this idea, we

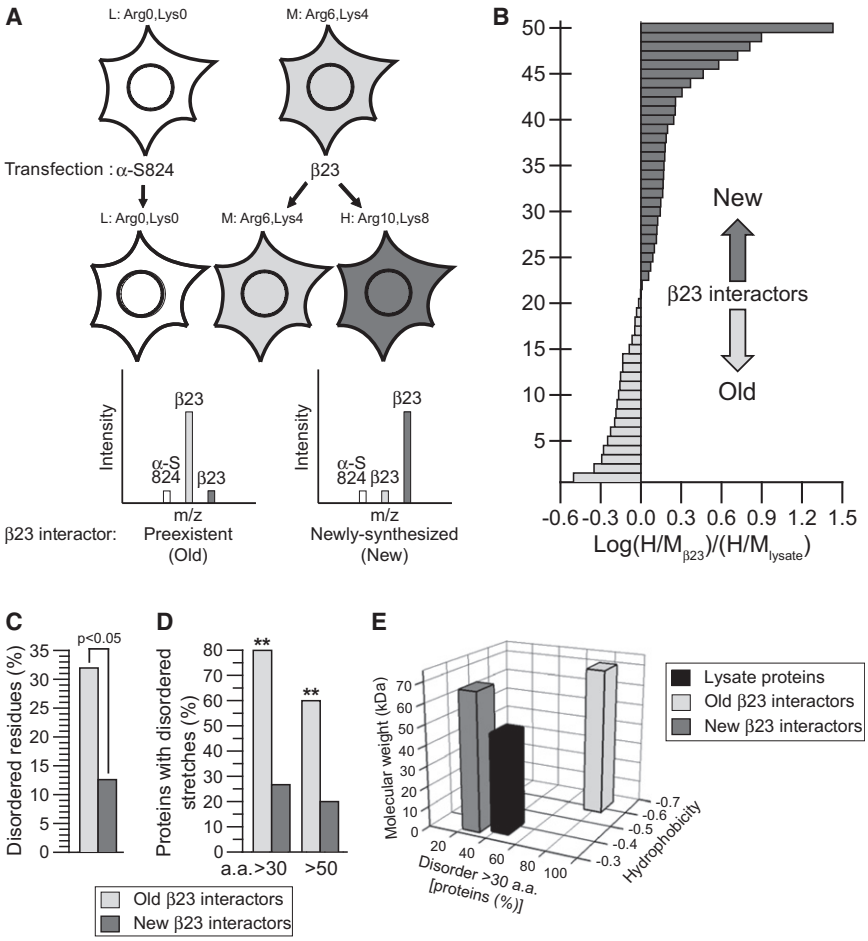

Figure 6. Newly Synthesized and Pre-Existent β Protein Interactors

(A) Design of SILAC based mass spectrometric analysis to identify proteins preferentially interacting with β23 as newly synthesized (new) or preexistent (old) proteins (Pulse-SILAC).

(B) Ratios of heavy to medium isotopes (H/M) of β23 interactors relative to the H/M ratios for the same proteins in the total cell lysate (see Extended Experimental Procedures). The log of this ratio of ratios increases with the tendency of a protein to interact with β23 as a new protein.

(C and D) Disorder analysis of new and old β23 interactors. Percentage of disordered residues in interactor sequences (C). p value is based on Mann-Whitney test. Fraction of proteins with continuous disordered stretches > 30 or > 50 amino acids (aa) (D). **$p < 0.005$ for old interactors relative to lysate (see Figure 5D), based on Chi-square test.

(E) Molecular weight, disorder and hydrophobicity of old and new β23 interactors relative to lysate proteins.

See also Figure S6 and Tables S4 and S7.

pulse-labeled HEK293T cells expressing β23 or α-S824 with ^{35}S-methionine, followed by immunoisolation of the proteins. Around 7% of the proteins labeled within 15 min were coisolated with β23, compared to only ~1% with α-S824 (Figure S6A), suggesting that a substantial fraction of newly synthesized polypeptides can interact with β23.

To identify such proteins, we performed pulse-SILAC experiments. Cells were cultured with medium amino acid isotopes (M) to label preexistent proteins, followed by transfection with β23. The culture was divided and one half was immediately shifted to media containing heavy amino acid isotopes (H). Control cells were cultured with light amino acids (L) and transfected with α-S824. After 24 hr, the cells from the three conditions were combined and subjected to anti-Myc pulldown and LC-MS/MS analysis (Figure 6A). The H/M isotope ratio of the β23 interactors in the pulldown relative to their H/M ratios in the lysate was used to indicate whether they interact with β23 preferentially as newly synthesized (New) or pre-existent (Old) proteins (Figure 6A). H/M labeling ratios were obtained for 50 β23 interactors, and a number of these showed a clear preference for interaction soon after synthesis (Figure 6B and Table S7). In contrast, fewer proteins interacted preferentially as old proteins. These interactors include Hsp110 as well as several translation initiation factors (Table S7), consistent with impairment of translation efficiency being an early consequence of β protein toxicity (Figures S3E–S3G).

Interestingly, the old and new interactors from the ends of the distribution (15 proteins each) differ markedly in their structural properties. The old interactors contain a significantly greater fraction of amino acids in IURs than the new interactors (Figure 6C). They are strongly enriched in continuous disordered regions (Figure 6D) and are of low average hydrophobicity (Figure 6E). In contrast, the new proteins are similar to lysate proteins in terms of hydrophobicity, but are lower in disorder and substantially larger in size (Figure 6E). Their folding pathways may be complex and kinetically slow, possibly resulting in the prolonged exposure of hydrophobic residues during folding. Based on analysis using the Z^{agg} algorithm, the new β23 interactors show high intrinsic aggregation scores only in their unfolded states (Figure S6B). In contrast, the old interactors are highly flexible and are unable to bury aggregation-prone regions in their native structures. Thus, these proteins have high aggregation scores both in their unfolded and folded states (Tartaglia et al., 2008) (Figure S6B). Some of them may coaggregate as preexistent or newly synthesized proteins, consistent with their lower peak values in the isotope labeling ratios compared to the new proteins (Figure 6B).

In summary, the β23 interactors can be divided into two overlapping subsets of relatively aggregation-prone proteins: One group is enriched in IURs, which would be prone to aggregate even in their post-folding state. This group is highly represented among the old proteins. The second group contains an abundance of large and/or multidomain proteins, which require longer times for synthesis and may fold slowly. Consequently, in

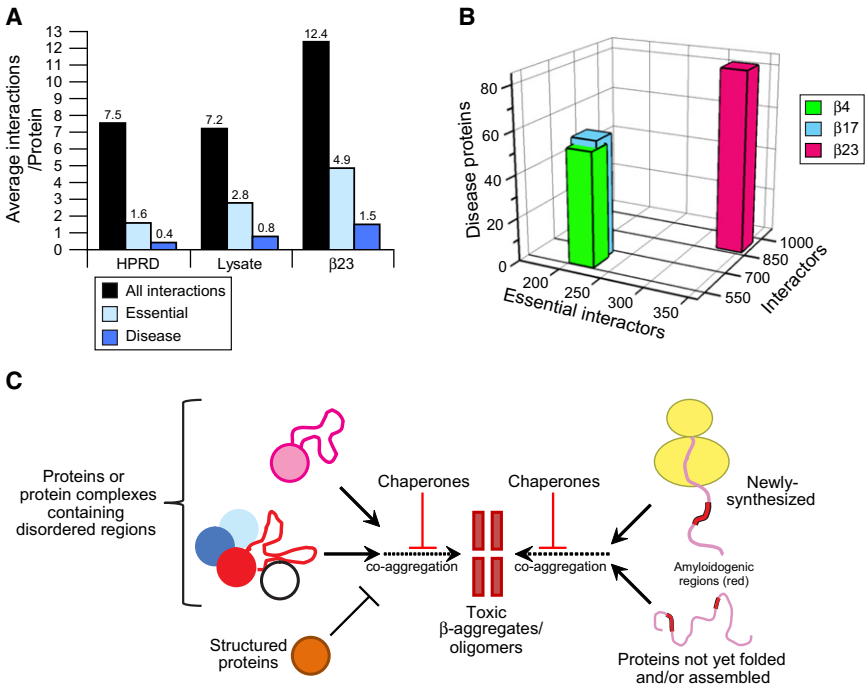

Figure 7. Mechanism of β Aggregation Toxicity

(A and B) Functional context of β protein interactors within the protein interaction network. Shown in (A) are the average number of functional interactions of the β23 interactors in comparison to proteins in the HPRD database and in the experimentally determined cell lysate (~3000 proteins). These functional interactions are categorized into total interactions, interactions with essential proteins and interactions with proteins involved in neurodegenerative disease (Raychaudhuri et al., 2009). In (B), the complete sets of β4, β17, and β23 interactors are compared in terms of these functional properties.

(C) Model for the interaction of β aggregates with pre-existent and newly synthesized proteins. Pre-existent proteins are structurally flexible in their functional state and are involved in multiple protein-protein interactions, which may be disrupted by their association with the β aggregates. The newly synthesized proteins are structurally vulnerable to coaggregation during folding and assembly. Interaction of both the preexistent and newly synthesized proteins with the β aggregates is facilitated by the limiting capacity of chaperones to shield aggregate surfaces and by the failure of the cells to mount an efficient stress response.

conditions of limited chaperone capacity, they would be prone to aggregate during and shortly after synthesis. This group is enriched among the newly synthesized proteins. Finally, some proteins occupy a transition zone, combining physicochemical features of both groups.

Aggregate Interactors Have Critical Network Functions

The structural flexibility and relatively large size of the aggregate interactors suggests that these proteins may normally be involved in numerous functional protein interactions. To address this possibility, we analyzed how the β23 interactors are linked with the cellular protein network. A query of the Human Proteome Reference Data Base (HPRD) (Keshava Prasad et al., 2009) revealed that each of these proteins functionally interacts with ~12 different proteins on average, compared to ~7 per lysate protein and ~7.5 per protein in HPRD (19,651 entries) (Figure 7A). Notably, most of the β23 interactors have no or only few interactions with any of the other β23 interactors, suggesting that coaggregation may disrupt their functional complexes. For example, the microfilament protein vimentin interacts with more than 100 different proteins according to HPRD, but only three of those are among the identified β23 interactors, although 49 potential vimentin interactors were detected in the lysate or background of the pulldowns (data not shown).

Essential proteins often occupy critical "hub" positions in the network (Haynes et al., 2006; Jeong et al., 2001). Each β23 target protein interacts on average with ~5 different essential proteins, compared to only ~3 per lysate protein and ~1.5 per entry in HPRD (Figure 7A). Moreover, the β23 interactors are more frequently linked than lysate proteins, through direct interactions, with proteins that have been found in association with neurodegenerative disease proteins (Raychaudhuri et al., 2009) (Figure 7A and Table S1).

Assuming that a disturbance of functional protein interactions contributes critically to β aggregation toxicity, β23 would be expected to differ in this regard from the less cytotoxic proteins β4 and β17. We found that the β4, β17 and β23 interactors are physically linked to a total of 600, 643, and 912 different proteins, including 216, 213, and 340 essential proteins and 53, 56, and 84 proteins associated with neurodegenerative disease networks, respectively (Figure 7B). Thus, the capacity of the β protein aggregates to interact with and sequester highly connected cellular proteins correlates well with their relative cytotoxicity.

DISCUSSION

Widespread Coaggregation of Metastable Proteins

A key finding of this study is that amyloidogenic aggregation can result in the sequestration of numerous proteins that share distinct physicochemical properties: They are relatively large in size and exhibit high structural flexibility, with a significant enrichment in disordered regions, features that are strongly linked with multifunctionality (Figure 7C).

The artificial β sheet proteins used as a model were designed to assemble into fibrils (West et al., 1999). Like natural amyloidogenic proteins, they populate a range of prefibrillar aggregation intermediates, which are likely to represent the primary toxic agents in aggregation diseases (Chiti and Dobson, 2006; Jahn and Radford, 2008). Based on recent findings, the proteotoxicity of such species correlates with the exposure of ANS-binding hydrophobic surfaces (Bolognesi et al., 2010; Campioni et al., 2010) and reactivity with the A11 anti-oligomer antibody

(Kayed et al., 2003), properties that are reproduced by the model proteins. Flexible hydrophobic surfaces and unpaired backbone structure that is not yet integrated into a stable cross-β core (Mossuto et al., 2010) may endow oligomers and protofilaments with the capacity to engage in widespread aberrant interactions with metastable proteins. Whether oligomeric species with similar interaction properties also occur during nonamyloidogenic aggregation, leading to amorphous structures rather than fibrils, remains to be determined.

The β protein aggregates were found to interact with preexistent and newly synthesized polypeptides (Figure 7C). The former are strongly enriched in intrinsically unstructured regions (IURs) and are of lower average hydrophobicity. A similar trend was observed for interactors of the toxic aggregates of the Arctic mutant of $A\beta_{1\text{-}42}$, which is known to transiently populate high concentrations of prefibrillar aggregates (Bolognesi et al., 2010) (Figures S5C–S5I). Proteins rich in structural disorder are considered to be adaptable to multiple interaction partners (Dunker et al., 2008; Pentony and Jones, 2009). On the other hand, local structural fluctuations in these proteins are expected to give rise to the exposure of sequence elements with a higher propensity to form aggregates, consistent with the relatively high Z^{agg} scores of the β protein interactors (Tartaglia et al., 2008). Indeed, some of the best known neurodegenerative disease proteins, such as α-synuclein or tau, are thought to be almost entirely unstructured. In contrast, the proteins that interact with the aggregates during or soon after synthesis have average hydrophobicity and disorder. These proteins tend to be large in size and are likely to populate nonnative states which expose hydrophobic surfaces during their folding, assembly or transport that must be shielded by molecular chaperones (Figure 7C). For example, among the β protein interactors are mitochondrial membrane proteins such as VDAC and the ADP/ATP translocase which require chaperone protection during post-translational sorting (Young et al., 2003).

By targeting flexible regions and hydrophobic surfaces of preexistent and newly synthesized proteins, the β protein aggregates may act in a 'chaperone-like' manner but cannot promote folding through regulated release. Consequently, more and more proteins are recruited, which in turn may generate new interaction surfaces, thereby magnifying the toxic potential of the aggregates ('snowball effect').

Interference with Multiple Key Cellular Functions

The β protein interactors include many proteins with key cellular functions in transcription and translation, chromatin regulation, vesicular transport, cell motility and architecture, as well as protein quality control (Figure 3C). Similar proteins were also found to interact with aggregates of Aβ (Table S5), suggesting that these pathways may be more generally at risk in aggregation disorders. Bioinformatic analysis showed that most of the coaggregating proteins have numerous functional interactors, consistent with their preferential role as network hubs (Haynes et al., 2006; Jeong et al., 2001). The number of functional interactions of the sequestered proteins correlates with the relative cytotoxicity of the β protein aggregates (Figure 7B). It is thus likely that the aggregates compete for binding to disordered regions with a protein's normal interactors and the more toxic forms may be able to compete more effectively. Based on our proteomic and biochemical measurements, ~10%–45% of total may be sequestered for several of the interacting proteins (Figures S3E–S3F and Table S1). Moreover, certain proteins may misfold upon interaction with the aggregates but remain in solution. Thus, dependent on the interaction strength of the aggregates, an increasing number of key functions may be affected, eventually resulting in fatal network collapse. We estimate that the human proteome contains ~2000 proteins that structurally resemble the experimentally identified β aggregate interactors. Dependent on cell type and the exact structural properties of the causative aggregate, different subsets of these proteins may be affected, which may help to explain different patterns of pathobiology. It will be interesting to see which of these proteins are preferentially targeted by β aggregates in neuronal cells.

Our results also lend support to the recent view that protein misfolding and aggregation disturbs proteostasis by compromising the cellular folding environment (Morimoto, 2008). We suggest that the association of endogenous proteins with the aggregates is facilitated by the failure of the affected cells to mount an efficient stress response, a phenomenon that was previously observed during prion infection (Tatzelt et al., 1995) and may be particularly serious in postmitotic cells, such as neurons. Inhibition of the stress response may be due to the sequestration by the aggregates of multiple chromatin regulators, which interact with numerous transcription factors, including HSF1 (Erkina et al., 2010; Sullivan et al., 2001). As a consequence of limiting proteostasis capacity, newly synthesized polypeptides with a high chaperone requirement for folding may become increasingly vulnerable to sequestration by disease protein aggregates (Figure 7C). This fatal chain of events may be further enhanced during aging, which is associated with a decline of proteostasis and thus would result in a reduced capacity of cells to protect their more vulnerable proteins against coaggregation (Balch et al., 2008; Morimoto, 2008).

EXPERIMENTAL PROCEDURES

Protein Purification and In Vitro Analysis of Aggregates

Proteins α-S824, β4, β17 and β23 were expressed in *E. coli* BL21 cells and purified as described in Extended Experimental Procedures. Fluorescence analysis, circular dichroism, FTIR spectroscopy and negative stain electron microscopy of the aggregates were performed using standard methods (see Extended Experimental Procedures).

Cell Culture, Immunoblotting and Reporter Assays

Human HEK293T cells were cultured under standard conditions (see Extended Experimental Procedures). Transient transfections were performed by electroporation with 30 μg expression vector or by Lipofectamin (Invitrogen) transfection for overexpression of Hsp110. Immunoblots were developed using the chemiluminescence kit Rodeo ECL (USB) and analyzed using a LAS-3000 image reader (Fujifilm) and the AIDA software (Raytest). For luciferase reporter assays, cells were lysed in Lysis Buffer (Promega) and luciferase activity measured using a Lumat LB9507 (EG&G Berthold).

Cell Viability

Cell viability was analyzed by measuring the capacity of cells to reduce 3-(4,5-Dimethylthiazol-2-yl)-2,5-diphenyltetrazoliumbromide (MTT) to formazan at different times after transfection with α-S824, β protein or $A\beta_{42}$-GFP constructs (Shearman, 1999).

Solubility Analysis and Oligomer Quantification

Cells were lysed in Triton X-100/Na deoxycholate-containing PBS with protease inhibitors. Benzonase was used to hydrolyze DNA. Raw debris was removed at 2000 × g for 5 min and the supernatant was fractionated by centrifugation (100.000 × g, 30 min) into pellet and soluble fractions or by gel filtration on a Superose 6 column (Amersham Bioscience), followed by dot blot analysis with anti-oligomer antibody A11 (Kayed et al., 2003) (see Extended Experimental Procedures for details).

Immunofluorescence and Fluorescence Imaging

Transfected cells were fixed with paraformaldehyde, permeabilized with Triton X-100 and stained with antibodies as indicated. Images were recorded with a Leica TCS SP2 confocal laser scanning microscope. Protein aggregates were analyzed by staining with NIAD-4 (ICX Nomadics) (see Extended Experimental Procedures).

SILAC and Sample Preparation for LC-MS/MS Analysis

Labeling of cells was performed in custom medium supplemented with light (L), medium (M) or heavy (H) arginine and lysine isotopes (see Extended Experimental Procedures). In pulse-SILAC experiments, M-labeled cells were shifted to H-medium, as indicated in Figure 6A. Cells were lysed and cell debris removed by low-speed centrifugation (2000 × g, 5 min). Lysates from L, M and H cells were adjusted to equal protein concentration and mixed at a 1:1:1 ratio. An aliquot of this mix was set aside as "lysate" control. Anti-Myc or anti-GFP MicroBeads (Miltenyi Biotech) were used to isolate the Myc-tagged proteins or GFP-fusion proteins and their interactors. The bound proteins were eluted and processed as described (Ong and Mann, 2006). The spectra were interpreted using MaxQuant version 1.0.12.31 (Cox and Mann, 2008) combined with Mascot version 2.2 (Matrix Science, www.matrixscience.com). See Extended Experimental Procedures for details. The raw MS data along with a full list of identified proteins and quantitations is available at https://proteomecommons.org/tranche, entering the following hash: +Ff0/p8lSBrrzCKZfzAwYS3+Bqw5fonokB679f136te2iklhHtFMUpeT5SM/l3XuufTyrXj0ycVVC6G4Li/L02 dA4jcAAAAAAABVfg = =.

Bioinformatic Analysis

Average hydrophobicity was calculated according to Kyte and Doolittle (1982), protein disorder using the DisoDB database (Pentony and Jones, 2009) and aggregation propensities according to Tartaglia et al. (2008). Protein fold prediction and the analysis of functional protein interactions are described in Extended Experimental Procedures. Student's t test and Mann-Whitney test were used to compare groups. Chi-square tests were used to determine significant differences between categorical data.

SUPPLEMENTAL INFORMATION

Supplemental information includes Extended Experimental Procedures, six figures, and seven tables and can be found with this article online at doi:10.1016/j.cell.2010.11.050.

ACKNOWLEDGMENTS

We thank C.G. Glabe for providing the A11 antibody and H. Wagner for plasmids HSP70-Luc and NF-κB-Luc. We acknowledge the help of H. Engelhardt with FTIR measurements, technical assistance by O. Mihalache and V. Marcus with electron microscopy, and R. Zenke (MPIB core facility) for confocal microscopy. Financial support from EU Framework 7 Integrated Project PROSPECTS, the Deutsche Forschungsgemeinschaft (SFB 596), the Ernst-Jung Foundation, and the Körber Foundation is acknowledged. H.O. and A.W. have a fellowship from the Fonds der Chemischen Industrie, and H.O. is supported by the Elite Graduate Network of Bavaria.

Received: April 15, 2010
Revised: September 6, 2010
Accepted: November 11, 2010
Published: January 6, 2011

REFERENCES

Balch, W.E., Morimoto, R.I., Dillin, A., and Kelly, J.W. (2008). Adapting proteostasis for disease intervention. Science *319*, 916–919.

Bence, N.F., Sampat, R.M., and Kopito, R.R. (2001). Impairment of the ubiquitin-proteasome system by protein aggregation. Science *292*, 1552–1555.

Bolognesi, B., Kumita, J.R., Barros, T.P., Esbjorner, E.K., Luheshi, L.M., Crowther, D.C., Wilson, M.R., Dobson, C.M., Favrin, G., and Yerbury, J.J. (2010). ANS Binding Reveals Common Features of Cytotoxic Amyloid Species. ACS Chem. Biol. *5*, 735–740.

Campioni, S., Mannini, B., Zampagni, M., Pensalfini, A., Parrini, C., Evangelisti, E., Relini, A., Stefani, M., Dobson, C.M., Cecchi, C., et al. (2010). A causative link between the structure of aberrant protein oligomers and their toxicity. Nat. Chem. Biol. *6*, 140–147.

Chiti, F., and Dobson, C.M. (2006). Protein misfolding, functional amyloid, and human disease. Annu. Rev. Biochem. *75*, 333–366.

Cooper, A.A., Gitler, A.D., Cashikar, A., Haynes, C.M., Hill, K.J., Bhullar, B., Liu, K.N., Xu, K.X., Strathearn, K.E., Liu, F., et al. (2006). Alpha-synuclein blocks ER-Golgi traffic and Rab1 rescues neuron loss in Parkinson's models. Science *313*, 324–328.

Cox, J., and Mann, M. (2008). MaxQuant enables high peptide identification rates, individualized p.p.b.-range mass accuracies and proteome-wide protein quantification. Nat. Biotechnol. *26*, 1367–1372.

Dosztanyi, Z., Csizmok, V., Tompa, P., and Simon, I. (2005). IUPred: web server for the prediction of intrinsically unstructured regions of proteins based on estimated energy content. Bioinformatics *21*, 3433–3434.

Dunker, A.K., Silman, I., Uversky, V.N., and Sussman, J.L. (2008). Function and structure of inherently disordered proteins. Curr. Opin. Struct. Biol. *18*, 756–764.

Erkina, T.Y., Zou, Y., Freeling, S., Vorobyev, V.I., and Erkine, A.M. (2010). Functional interplay between chromatin remodeling complexes RSC, SWI/SNF and ISWI in regulation of yeast heat shock genes. Nucleic Acids Res. *38*, 1441–1449.

Frydman, J. (2001). Folding of newly translated proteins in vivo: The role of molecular chaperones. Annu. Rev. Biochem. *70*, 603–647.

Gidalevitz, T., Ben-Zvi, A., Ho, K.H., Brignull, H.R., and Morimoto, R.I. (2006). Progressive disruption of cellular protein folding in models of polyglutamine diseases. Science *311*, 1471–1474.

Goldschmidt, L., Teng, P.K., Riek, R., and Eisenberg, D. (2010). Identifying the amylome, proteins capable of forming amyloid-like fibrils. Proc. Natl. Acad. Sci. USA *107*, 3487–3492.

Hartl, F.U., and Hayer-Hartl, M. (2002). Molecular chaperones in the cytosol: from nascent chain to folded protein. Science *295*, 1852–1858.

Haynes, C., Oldfield, C.J., Ji, F., Klitgord, N., Cusick, M.E., Radivojac, P., Uversky, V.N., Vidal, M., and Iakoucheva, L.M. (2006). Intrinsic disorder is a common feature of hub proteins from four eukaryotic interactomes. PLoS Comput. Biol. *2*, e100.

Jahn, T.R., and Radford, S.E. (2008). Folding versus aggregation: Polypeptide conformations on competing pathways. Arch. Biochem. Biophys. *469*, 100–117.

Jeong, H., Mason, S.P., Barabasi, A.L., and Oltvai, Z.N. (2001). Lethality and centrality in protein networks. Nature *411*, 41–42.

Kayed, R., Head, E., Thompson, J.L., McIntire, T.M., Milton, S.C., Cotman, C.W., and Glabe, C.G. (2003). Common structure of soluble amyloid oligomers implies common mechanism of pathogenesis. Science *300*, 486–489.

Keshava Prasad, T.S., Goel, R., Kandasamy, K., Keerthikumar, S., Kumar, S., Mathivanan, S., Telikicherla, D., Raju, R., Shafreen, B., Venugopal, A., et al. (2009). Human Protein Reference Database–2009 update. Nucleic Acids Res. *37*, D767–D772.

Kim, W., Kim, Y., Min, J., Kim, D.J., Chang, Y.T., and Hecht, M.H. (2006). A high-throughput screen for compounds that inhibit aggregation of the Alzheimer's peptide. ACS Chem. Biol. *1*, 461–469.

Kyte, J., and Doolittle, R.F. (1982). A simple method for displaying the hydropathic character of a protein. J. Mol. Biol. *157*, 105–132.

Lam, Y.C., Bowman, A.B., Jafar-Nejad, P., Lim, J., Richman, R., Fryer, J.D., Hyun, E.D., Duvick, L.A., Orr, H.T., Botas, J., et al. (2006). ATAXIN-1 interacts with the repressor Capicua in its native complex to cause SCA1 neuropathology. Cell *127*, 1335–1347.

Lashuel, H.A., and Lansbury, P.T., Jr. (2006). Are amyloid diseases caused by protein aggregates that mimic bacterial pore-forming toxins? Q. Rev. Biophys. *39*, 167–201.

Lee, E.K., Park, Y.W., Shin, D.Y., Mook-Jung, I., Yoo, Y.J., Lee, E.K., Park, Y.W., Shin, D.Y., Mook-Jung, I., and Yoo, Y.J. (2006). Cytosolic amyloid-beta peptide 42 escaping from degradation induces cell death. Biochem. Biophys. Res. Commun. *344*, 471–477.

Linding, R., Jensen, L.J., Diella, F., Bork, P., Gibson, T.J., and Russell, R.B. (2003). Protein disorder prediction: implications for structural proteomics. Structure *11*, 1453–1459.

Morimoto, R.I. (2008). Proteotoxic stress and inducible chaperone networks in neurodegenerative disease and aging. Genes Dev. *22*, 1427–1438.

Mossuto, M.F., Dhulesia, A., Devlin, G., Frare, E., Kumita, J.R., de Laureto, P.P., Dumoulin, M., Fontana, A., Dobson, C.M., and Salvatella, X. (2010). The Non-Core Regions of Human Lysozyme Amyloid Fibrils Give Rise to Cytotoxicity. J. Mol. Biol. *402*, 783–796.

Nesterov, E.E., Skoch, J., Hyman, B.T., Klunk, W.E., Bacskai, B.J., and Swager, T.M. (2005). In vivo optical imaging of amyloid aggregates in brain: design of fluorescent markers. Angew. Chem. Int. Ed. *44*, 5452–5456.

Nilsberth, C., Westlind-Danielsson, A., Eckman, C.B., Condron, M.M., Axelman, K., Forsell, C., Stenh, C., Luthman, J., Teplow, D.B., Younkin, S.G., et al. (2001). The 'Arctic' APP mutation (E693G) causes Alzheimer's disease by enhanced Abeta protofibril formation. Nat. Neurosci. *4*, 887–893.

Ong, S.E., and Mann, M. (2006). A practical recipe for stable isotope labeling by amino acids in cell culture (SILAC). Nat. Protoc. *1*, 2650–2660.

Pentony, M.M., and Jones, D.T. (2009). Modularity of intrinsic disorder in the human proteome. Proteins *78*, 212–221.

Raychaudhuri, S., Dey, S., Bhattacharyya, N.P., and Mukhopadhyay, D. (2009). The role of intrinsically unstructured proteins in neurodegenerative diseases. PLoS ONE *4*, e5566.

Shearman, M.S. (1999). Toxicity of protein aggregates in PC12 cells: 3-(4,5-dimethylthiazol-2-yl)-2,5-diphenyltetrazolium bromide assay. Methods Enzymol. *309*, 716–723.

Stefani, M., and Dobson, C.M. (2003). Protein aggregation and aggregate toxicity: new insights into protein folding, misfolding diseases and biological evolution. J. Mol. Med. *81*, 678–699.

Su, A.I., Cooke, M.P., Ching, K.A., Hakak, Y., Walker, J.R., Wiltshire, T., Orth, A.P., Vega, R.G., Sapinoso, L.M., Moqrich, A., et al. (2002). Large-scale analysis of the human and mouse transcriptomes. Proc. Natl. Acad. Sci. USA *99*, 4465–4470.

Sullivan, E.K., Weirich, C.S., Guyon, J.R., Sif, S., and Kingston, R.E. (2001). Transcriptional activation domains of human heat shock factor 1 recruit human SWI/SNF. Mol. Cell. Biol. *21*, 5826–5837.

Tartaglia, G.G., Pawar, A.P., Campioni, S., Dobson, C.M., Chiti, F., and Vendruscolo, M. (2008). Prediction of aggregation-prone regions in structured proteins. J. Mol. Biol. *380*, 425–436.

Tatzelt, J., Zuo, J., Voellmy, R., Scott, M., Hartl, F.U., Prusiner, S.B., and Welch, W.J. (1995). Scrapie prions selectively modify the stress response in neuroblastoma cells. Proc. Natl. Acad. Sci. USA *92*, 2944–2948.

Wei, Y.N., Liu, T., Sazinsky, S.L., Moffet, D.A., Pelczer, I., and Hecht, M.H. (2003). Stably folded de novo proteins from a designed combinatorial library. Protein Sci. *12*, 92–102.

West, M.W., Wang, W.X., Patterson, J., Mancias, J.D., Beasley, J.R., and Hecht, M.H. (1999). De novo amyloid proteins from designed combinatorial libraries. Proc. Natl. Acad. Sci. USA *96*, 11211–11216.

Williams, G.T., McClanahan, T.K., and Morimoto, R.I. (1989). E1a transactivation of the human HSP70 promoter is mediated through the basal transcriptional complex. Mol. Cell. Biol. *9*, 2574–2587.

Winklhofer, K.F., Tatzelt, J., and Haass, C. (2008). The two faces of protein misfolding: gain- and loss-of-function in neurodegenerative diseases. EMBO J. *27*, 336–349.

Young, J.C., Hoogenraad, N.J., and Hartl, F.U. (2003). Molecular chaperones Hsp90 and Hsp70 deliver preproteins to the mitochondrial import receptor Tom70. Cell *112*, 41–50.